Intensity modulation response of injection-locked quantum cascade lasers

Cheng Wang[a*], Frédéric Grillot[b] and Jacky Even[a]

[a]Université Européenne de Bretagne, INSA, CNRS FOTON, 20 avenue des buttes de Coesmes, 35708 Rennes Cedex 7, France
[b]Telecom Paristech, Ecole Nationale Supérieure des Télécommunications, CNRS LTCI, 46 rue Barrault, 75013 Paris, France

ABSTRACT

The intensity modulation (IM) property of an optical injection-locked quantum cascade (QC) laser is theoretically investigated via a three-level rate equation model. The locking regime is obtained based on the local bifurcation theory. It is shown that the injection-locked QC laser exhibits a rather flat modulation response at zero detuning, whose bandwidth increases with the injection level. In contrast to interband lasers, both positive and negative detunings enhance the modulation bandwidth. Besides, a large linewidth enhancement factor (LEF) can increase the peak amplitude in the response. Moreover, it is found that no frequency dip occurs in the IM response of injection-locked QC lasers.

Keywords: quantum cascade laser, injection locking, nonlinear dynamics, modulation response

1. INTRODUCTION

Quantum cascade (QC) lasers have progressed very rapidly since its first demonstration at Bell Labs in 1994 [1]. One fundamental feature of the QC laser is that the laser radiation is based on intersubband transition, typically in the conduction band, which is dominated by electron-optical phonon scattering. The unique intersubband transition leads to a wide wavelength ranging from mid-infrared up to terahertz (3 μm–1000 μm), which is tailored by the quantum confinement. The electron-optical phonon scattering is an ultrafast relaxation mechanism in the order of several picoseconds, which makes QC lasers much more favorable for ultra-high-speed modulation [2-5]. In contrast, conventional semiconductor lasers rely on interband transitions, which take place between the conduction band and the valence band. The emission wavelength is located within a small range determined by the material bandgap. Besides, the interband transition is dominated by the carrier-carrier scattering mechanism, resulting in a longer carrier lifetime in the order of a few nanoseconds. Then, the modulation bandwidth of interband lasers is typically limited to less than 10 GHz [6]. In order to boost the modulation properties, researchers resort to the optical injection-locking technique, and it was demonstrated that the bandwidth of interband lasers can be strongly enhanced. Moreover, injection locking is beneficial to reduce the frequency chirp [7], [8], to suppress the relative intensity noise (RIN) [9], [10] and the nonlinear distortion [11]-[13]. It is well known that the injection-locked semiconductor laser's frequency response is characterized by three regimes depending on the frequency detuning. As shown in figure 1, for the negative frequency detuning the laser exhibits a linear response without resonance peak, while at zero detuning the laser is characterized by a broadband and flat response. At positive frequency detuning, the laser exhibits an even higher resonance frequency with a large peak, nevertheless, the modulation bandwidth is limited by the occurrence of the large pre-resonance frequency dip. It is proposed that the enhanced resonance frequency of the injection locked semiconductor lasers originates from the interference between the locked field and the shifted cavity-resonance field [14]-[16], while in the free-running case the relaxation oscillation results from the interaction between carriers and photons.

Regarding the picosecond carrier lifetime of QC lasers, a modulation bandwidth of more than 100 GHz was theoretically predicted [2-5]. It is noted that the bandwidth is also related to the photon lifetime, which is comparable or even larger than the carrier lifetime [17]-[19]. Experimentally, tens of gigahertz bandwidth was reported in the modulation response of QC lasers [20]-[22]. Due to the ultrafast carrier lifetime, it is also stressed that no relaxation oscillation resonance appears in the frequency response since the laser is over-damped [19]. As for injection-locked interband semiconductor lasers, it is beneficial to employ the injection locking technique to enhance the dynamical properties of QC lasers.

* cheng.wang@insa-rennes.fr; phone +33 223238464;

Physics and Simulation of Optoelectronic Devices XXI, edited by Bernd Witzigmann, Marek Osinski, Fritz Henneberger, Yasuhiko Arakawa, Proc. of SPIE Vol. 8619, 86191Q · © 2013 SPIE
CCC code: 0277-786X/13/$18 · doi: 10.1117/12.2002007

To this end, Meng *et al* theoretically investigated the injection-locking properties employing a simplified two-level rate equation model. It was shown that the bandwidth can be up to ~10-fold improved with a 10 dB injection ratio in comparison to the free-running case. One of the most interesting results is the absence of the unstable locking region in an approximate locking regime determined by the gain and phase condition [23]. However, at this stage we believe that this result needs further investigation via a more explicit analysis approach of the locking diagram such as numerical continuation. Moreover, a direct link of a mid-infrared QCL to a frequency comb using the optical injection technique has been demonstrated recently by Borri *et al* [24]. To go a step beyond Meng's work, this paper theoretically investigated the intensity modulation (IM) properties of an injection-locked QC laser employing a three-level rate equation model. The injection-locked regime is studied based on the local bifurcation theory. As for interband lasers, the locking regime is enlarged under high injection ratio. The QC laser exhibits a rather flat modulation response under zero detuning, whose bandwidth increases with the injection level. Both positive and negative frequency detunings can enhance the 3-dB bandwidth and the peak amplitude. The latter can also arise with a large linewidth enhancement factor (LEF). Moreover, it is found that no frequency dip occurs in the modulation response of injection-locked QC lasers.

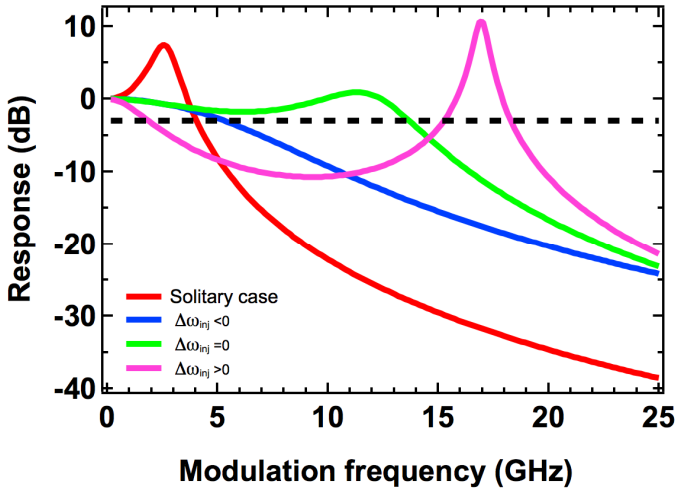

Figure 1. Modulation responses of optical injection-locked interband lasers at negative frequency detuning (blue), zero detuning (green) and positive frequency detuning (pink).

2. NUMERICAL MODEL DESCRIPTION

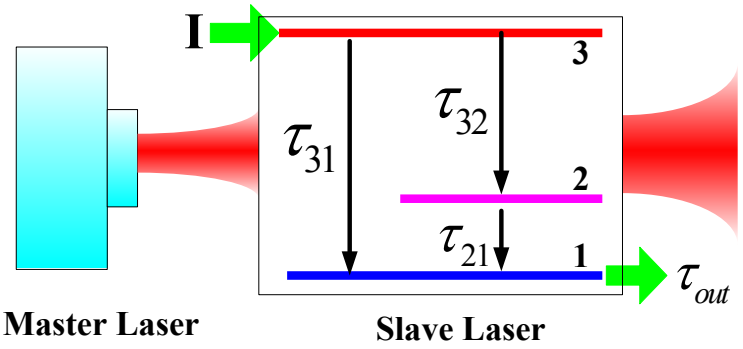

Figure 2. Sketch of optical injection-locked QCL laser and carrier dynamics in the slave laser

The schematic structure of optical injection-locked QC laser as well as the carrier dynamics is illustrated in figure 2. In the slave laser, carriers are firstly injected into the upper subband (labelled 3) of the active region by resonant tunnelling, and the tunnelling time from the injector is ignored since it is extremely short (~0.2ps) [1]. Laser radiation occurs through the carrier transition from the upper subband to the lower subband (labelled 2) within a relaxation time τ_{32}, and the relaxation mechanism is dominated by electron-optical phonon scattering. Meanwhile some carriers relax directly into the bottom state (labelled 1) within time τ_{31}. Once carriers are in the lower subband, those relax into the bottom

state via the emission of a longitudinal-optical (LO) phonon, and then tunnel out of the active region into the next stage within time τ_{out}. We note that only one period is considered in our model as in reference [5]. It is well known that the classical equation describing the complex field of an injection-locked laser is as follows [25]:

$$\frac{dE(t)}{dt} = \frac{1}{2}\left(G - \frac{1}{\tau_P}\right)(1 + j\alpha_H)E(t) + k_c A_{inj} - j\Delta\omega_{inj}E(t) \tag{1}$$

where $E(t)$ is the slave laser's complex field, G is the gain, τ_P is the photon lifetime, A_{inj} is the injected field magnitude, α_H is the LEF, $\Delta\omega_{inj}$ is the detuning frequency defined as $\Delta\omega_{inj} = \omega_{master} - \omega_{slave}$ while k_c is the coupling rate of the master laser into the slave laser which is $k_c = c(1-R)/(2n_r L\sqrt{R})$ with n_r the refractive index and L is the cavity length. The complex rate equation (1) can be split into two coupled rate equations for the photon number S and the phase $\Delta\phi$, according to the relationship $E(t) = \sqrt{S(t)}\exp j\Delta\phi(t)$ with the phase difference $\Delta\phi = \phi_{slave} - \phi_{master}$. The injection ratio is defined as $R_{inj}=S_{inj}/S_{FE}$ with the free-running photon number S_{FE}. Following the sketch of Figure 2 and the rate equation model of free running QC lasers reported in references [26]-[28], the rate equations for optical injection-locked QCLs are finally given by:

$$\frac{dN_3}{dt} = \frac{I}{q} - \frac{N_3}{\tau_{32}} - \frac{N_3}{\tau_{31}} - G_0\Delta NS \tag{2}$$

$$\frac{dN_2}{dt} = \frac{N_3}{\tau_{32}} - \frac{N_2}{\tau_{21}} + G_0\Delta NS \tag{3}$$

$$\frac{dN_1}{dt} = \frac{N_3}{\tau_{31}} + \frac{N_2}{\tau_{21}} - \frac{N_1}{\tau_{out}} \tag{4}$$

$$\frac{dS}{dt} = \left(G_0\Delta N - 1/\tau_P\right)S + \beta\frac{N_3}{\tau_{sp}} + 2k_c\sqrt{S_{inj}S}\cos\Delta\phi \tag{5}$$

$$\frac{d\Delta\phi}{dt} = \frac{\alpha_H}{2}\left(G_0\Delta N - 1/\tau_P\right) - \Delta\omega_{inj} - k_c\sqrt{\frac{S_{inj}}{S}}\sin\Delta\phi \tag{6}$$

where I is the pump current, $N_{3,2,1}$ are the carrier numbers in levels 3, 2, 1, respectively. The gain $G = G_0\Delta N$ with the gain coefficient G_0 and $\Delta N = N_3 - N_2$. τ_P is the photon lifetime, τ_{sp} is the spontaneous emission time and β is the spontaneous emission factor.

In order to obtain the modulation transfer function, we linearize the rate equations (2)-(6). Assuming a small current deviation i around the pump current I, the deviations of $N_{3,2,1}$, S, $\Delta\phi$ are defined as $n_{3,2,1}$, s and $\delta\varphi$, respectively. Then we can obtain the differential rate equations as follows:

$$\begin{bmatrix} \gamma_{11}+j\omega & -\gamma_{12} & 0 & -\gamma_{14} & 0 \\ -\gamma_{21} & \gamma_{22}+j\omega & 0 & -\gamma_{24} & 0 \\ -\gamma_{31} & -\gamma_{32} & \gamma_{33}+j\omega & 0 & 0 \\ -\gamma_{41} & -\gamma_{42} & 0 & \gamma_{44}+j\omega & -\gamma_{45} \\ -\gamma_{51} & -\gamma_{52} & 0 & -\gamma_{54} & \gamma_{55}+j\omega \end{bmatrix} \begin{bmatrix} n_3 \\ n_2 \\ n_1 \\ s \\ \delta\varphi \end{bmatrix} = \frac{i}{q}\begin{bmatrix} 1 \\ 0 \\ 0 \\ 0 \\ 0 \end{bmatrix} \tag{7}$$

with

$$\gamma_{11}=G_0S+\frac{1}{\tau_{32}}+\frac{1}{\tau_{31}};\quad \gamma_{12}=G_0S;\quad \gamma_{14}=-G_0\Delta N;\quad \gamma_{21}=G_0S+\frac{1}{\tau_{32}};$$
$$\gamma_{22}=G_0S+\frac{1}{\tau_{21}};\quad \gamma_{24}=G_0\Delta N;\quad \gamma_{31}=\frac{1}{\tau_{31}};\quad \gamma_{32}=\frac{1}{\tau_{21}};\quad \gamma_{33}=\frac{1}{\tau_{out}};$$
$$\gamma_{41}=G_0S+\frac{\beta}{\tau_{sp}};\quad \gamma_{42}=-G_0S;\quad \gamma_{44}=\frac{1}{\tau_P}-G_0\Delta N-k_c\cos\phi\sqrt{\frac{S_{inj}}{S}};\tag{8}$$
$$\gamma_{45}=-2k_c\sin\phi\sqrt{S_{inj}S};\quad \gamma_{51}=\frac{\alpha_H}{2}G_0;\quad \gamma_{52}=-\frac{\alpha_H}{2}G_0;$$
$$\gamma_{54}=\frac{k_c\sin\phi}{2S}\sqrt{\frac{S_{inj}}{S}};\quad \gamma_{55}=k_c\cos\phi\sqrt{\frac{S_{inj}}{S}}$$

Then, the modulation transfer function can be extracted as

$$H(\omega)=\frac{s(\omega)/i(\omega)}{s(0)/i(0)}=\frac{p_1p_2p_3p_4p_5}{z_1z_2z_3}\frac{\prod_{k=1}^{3}(j\omega-z_k)}{\prod_{k=1}^{5}(j\omega-p_k)}\tag{9}$$

where z_k is the zero, while p_k is the pole which is also eigenvalue of the coefficient matrix in the differential rate equation. The poles and zeros are useful for the behaviour analysis of the modulation response with respect to the Bode plot. Besides, the eigenvalues are also important for the stability analysis in the bifurcation diagram, which will be discussed in the following sections.

Table 1. The QD material parameters and the laser parameters used in the simulations (from [28]-[30])

Parameter	Value	Parameter	Value
Laser frequency ν	2.9 THz	Relaxation time τ_{32}	2.0 ps
Cavity length L	3 mm	Relaxation time τ_{31}	2.4 ps
Cavity width w	80 μm	Relaxation time τ_{21}	0.5 ps
Facet reflectivity R	0.29	Tunnelling out time τ_{out}	0.5 ps
Refractive index n_g	3.3	Photon lifetime τ_P	3.7 ps
Internal loss α_i	24 cm^{-1}	Spontaneous lifetime τ_{sp}	7.0 ns
Gain coefficient G0	5.3×10^4 s^{-1}	LEF α_H	0.5

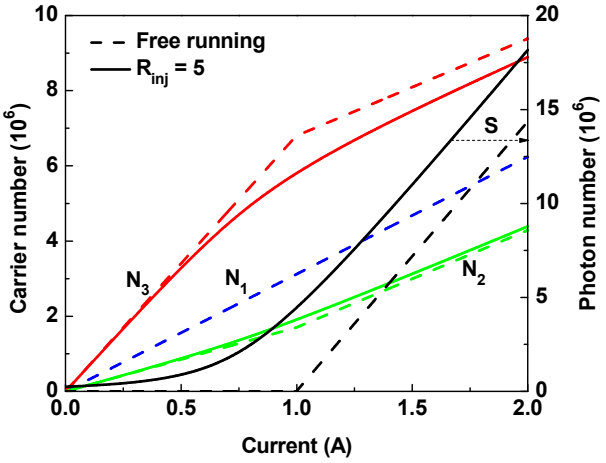

Figure 3. Steady-state results for an injection-locked QC laser (solid lines) with an injection ratio R_{inj}=5 at zero detuning, in comparison with the free-running case (dashed lines).

3. RESULTS AND DISCUSSIONS

All the material and laser parameters used in our simulations are listed in table 1(unless stated otherwise) [28]-[30]. As shown in figure 3, we firstly studied the steady-state properties of the injection-locked QC laser with an injection ratio R_{inj}=5 under the zero detuning case. The laser's threshold for the free-running laser is I_{th}=1 A. In comparison with the free-running case, the carrier number N_3 in the upper laser state is reduced while N_2 in the lower laser state is increased by optical injection. Nevertheless, the carrier number in the bottom state, which is $N_1 = \tau_{out} I / q$ is not impacted as in the free-running case. Moreover, we note that the photon number is enhanced by the optical injection as well. In the following sections the bias current is set at I_{bias} =1.2I_{th}.

In order to obtain the stable injection-locking regime we studied the local bifurcations, namely saddle-node (also called limit point or fold) and Hopf bifurcations [31], [32]. The bifurcations can be obtained by an eigenvalue analysis of the fixed point (or equilibrium), that is, if a single, real eigenvalue passes through the imaginary axis in the complex plane, one typically finds a saddle-node bifurcation while a pair of complex conjugate eigenvalues passing through the imaginary axis corresponds to a Hopf bifurcation. The bifurcations can be calculated by the so-called numerical continuation, which is a powerful method for bifurcation analysis, and it is implemented by the continuation package Matcont in our work. The saddle-node (SN, solid line) and Hopf (dashed line) bifurcations are illustrated in figure 4. The stable locking regime is bounded by the supercritical bifurcations (thick lines). As for injection-locked interband lasers, the injection-locked regime enlarges with the injection ratio. It is also well known that the bifurcation diagram has a strong dependence on the LEF as is compared between figure 4(a) and (b). With a large LEF value, the stable locking regime is enlarged both at the positive frequency detuning edge and the negative frequency detuning edge. It is noted that there are codimension-two points (G_1, G_2) where the Hopf and SN curves intersect, and the bifurcations changes from supercritical (subcritial) to subcritical (supercritical) along both the Hopf and SN curves [31], [32]. Near the point G_1, the laser is known to generate various nonlinear dynamics. In comparison with interband lasers, the positions of the codimension-two points move to a higher injection level.

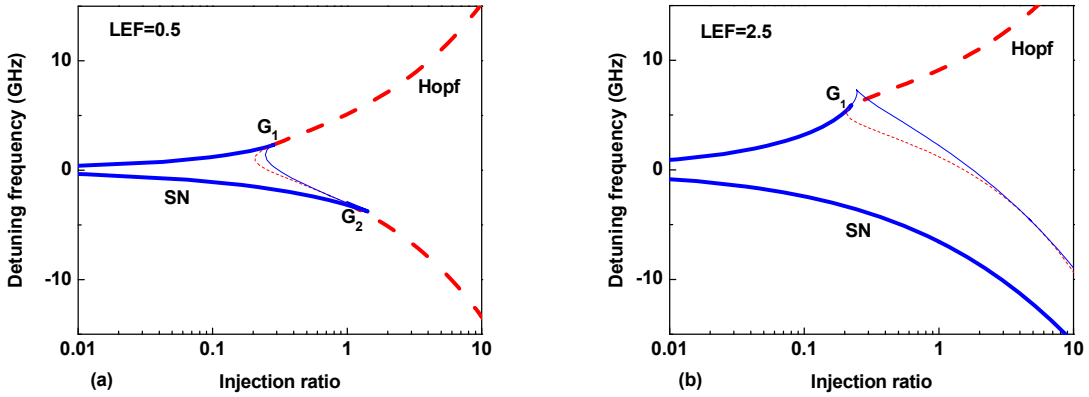

Figure 4. Bifurcation diagram and stable locking regime of an injection-locked QC laser. Solid line is saddle-node (SN) bifurcation and dashed line is Hopf bifurcation. Supercritical bifurcation is denoted by thick line while subcritical bifurcation by thin line. The stable locking regime is bounded by the supercritical bifurcations with (a) LEF=0.5, and (b) LEF=2.5.

Figure 5(a) shows effects of the injection strength on the modulation response of the injection-locked QC laser at zero detuning. As for the free-running laser, the injection-locked laser exhibits a rather flat response without resonance peak due to its ultrafast carrier lifetime. As is illustrated in figure 5(b), the 3-dB bandwidth increases with the injection level. The bandwidth at R_{inj}=10 is 31.7 GHz corresponding to about 2.5-fold improvement as compared to the free-running case (12.8 GHz).

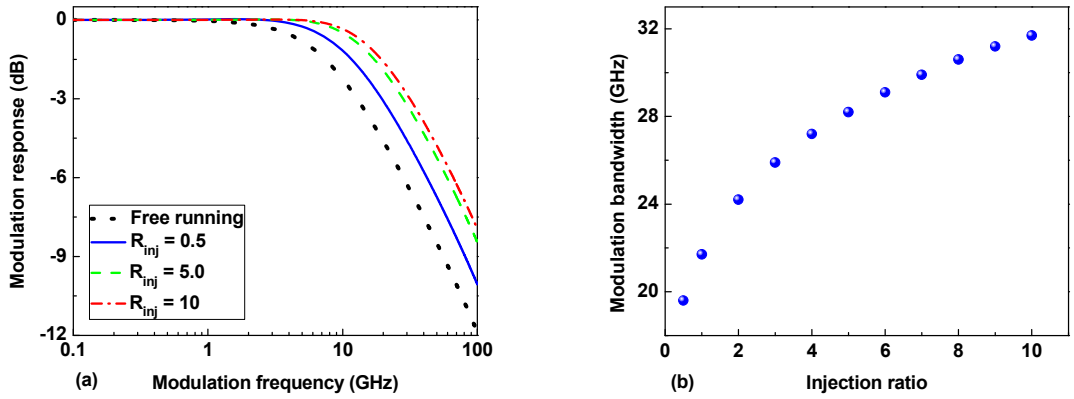

Figure 5. (a) Modulation response with various injection ratios at zero detuning; (b) 3-dB bandwidth as a function of injection ratio.

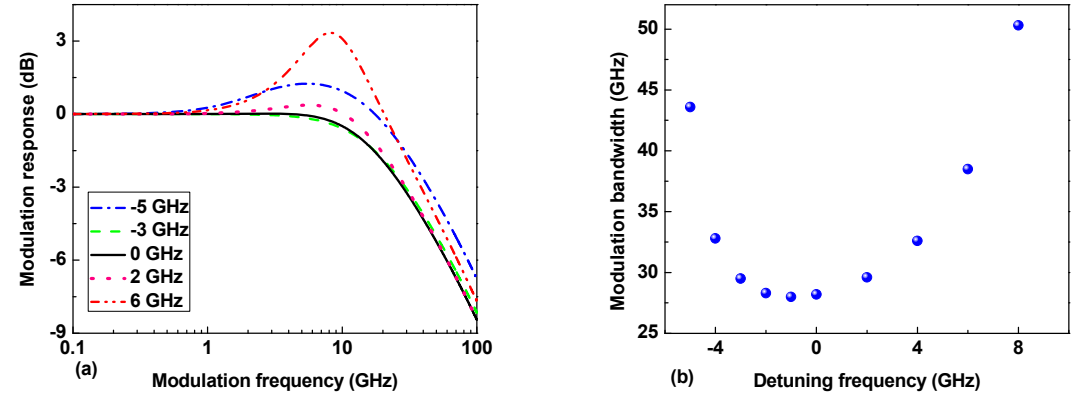

Figure 6. (a) Modulation response under various detuning frequencies at an injection ratio of R_{inj}= 5; (b) Modulation bandwidth as a function of detuning frequency.

Table 2. Poles and zeroes for various detuning frequencies in figure 6(a)

Detuning	p_1	p_2	p_3	p_4	p_5	z_1	z_2	z_3
-5 GHz	-18.3	-99.2	-1016.7	-2492.6	-2000	-12.1	-1500	-2000
-3 GHz	-25.4	-106.4	-1028.7	-2583.1	-2000	-24.9	-1500	-2000
0 GHz	-35.7	-90.6	-1024.7	-2550.5	-2000	-32.07	-1500	-2000
2 GHz	-56.0±j10.6		-1013.5	-2467.6	-2000	-32.09	-1500	-2000
6 GHz	-30.9±j45.1		-978.4	-2257.3	-2000	-24.7	-1500	-2000

Figure 6(a) presents the impacts of the frequency detuning on the modulation response. In contrast to the interband lasers in figure 1, peak arises when the frequency detunes toward both the positive (6 GHz) and the negative (-5 GHz) locking edge. However, the occurrence of the peak is not because of the relaxation oscillation resonance. It can be analyzed via the poles and zeroes listed in table 2 with respect to the Bode plot. The parameters p_1, p_2 and z_1 are dominant in the modulation response since other poles and zeroes are much larger. The peak appearance is attributed to the fact that the zero $|z_1|$ is smaller than the smallest pole $|p_1|$, since the larger the value $|p_1|$ - $|z_1|$ is, the higher the peak becomes. At positive detuning, the small real part of the complex poles also contributes to the peak occurrence. In comparison with the modulation response of interband lasers under positive frequency detuning in Figure 1, no frequency dip occurs in the modulation response of the QC laser due to the small zero $|z_1|$ value, which is a crucial point for broadband application of QC lasers. Figure 6(b) illustrates the variation of the modulation bandwidth under frequency detuning. In

contrast to interband lasers the bandwidth increases both for positive and negative detunings, and the smallest value is reached around the detuning frequency at -1 GHz.

Although QC lasers are theoretically predicted to exhibit a near-zero LEF because of the near-homogeneously broadened gain spectrum, recent experiments have shown that the above-threshold LEF of QC lasers can actually range from 0 to 2.5 [19], [33]-[35]. Correspondingly, we studied the influence of the LEF on the modulation response in figure 7. With a large LEF value, the peak amplitude increases while the modulation bandwidth is nearly unchanged. So it is beneficial to maintain a low LEF value to obtain a relatively flat modulation response.

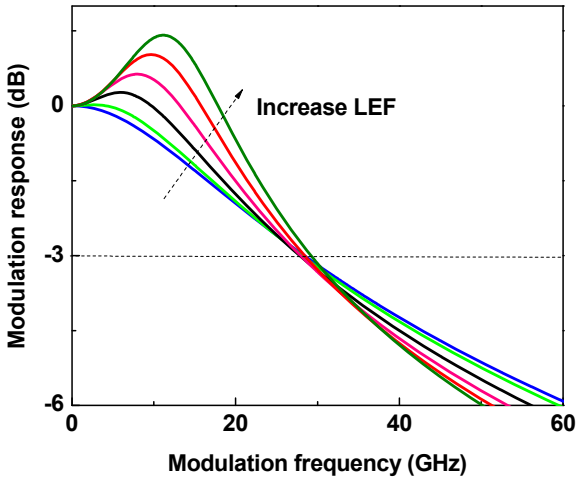

Figure 7. Modulation response at zero detuning with R_{inj}=5 under various LEF values LEF=0.1, 0.5, 1.0, 1.5, 2.0, 2.5.

4. CONCLUSION

Based on a set of five rate equations, the modulation properties of an injection-locked QC laser are theoretically studied via a semi-analytical method. The injection-locking regime is obtained through the local bifurcation theory including saddle-node and Hopf bifurcations. It is shown that the QC laser exhibits a rather flat modulation response under zero detuning, and that the modulation bandwidth increases with the injection strength. In comparison with injection-locked interband lasers, it is demonstrated that both positive and negative detunings enhance the modulation bandwidth. Furthermore, it is also found that no frequency dip occurs in the IM response, which is extremely beneficial for broadband applications of QC lasers. Lastly, large LEF value can increase the peak amplitude in the modulation response. These results are of prime importance for the enhancement of QC lasers' dynamical properties. Further study will take into account the period of stages to improve the rate equation model. The influence of the carrier lifetimes on the injection-locked properties will be investigated as well.

ACKNOWLEDGMENTS

The authors would like to thank Professor Carlo Sirtori and Dr. S. Barbieri of Université Paris Diderot-Paris 7, France as well as Professor Thomas Erneux from Brussels University Belgium for helpful discussions. Dr. Frédéric Grillot's work is supported in part by the European Office of Aeorospace Research and Development (EOARD) under grant FA8655-12-1-2093. Cheng Wang's work is supported by China Scholarship Council.

REFERENCES

[1] Faist, J., Capasso, F., Sivco, D. L., Sirtori, C., Hutchinson, A. L., and Cho, A. Y., "Quantum cascade laser," Science 264, 553-556 (1994).

[2] Mustafa, N., Pesquera, L., Cheung, C. Y. L., and Shore, K. A., "Terahertz bandwidth prediction for amplitude modulation response of unipolar intersubband semiconductor lasers," IEEE Photon. Technol. Lett. 11(5), 527-529 (1999).

[3] Cheung, C. Y. L., Spencer, P. S., and Shore K. A., "Modulation bandwidth optimization for unipolar intersubband semiconductor lasers," IEEE proceedings Optoelectronics 144(1), 44-47 (1997).

[4] Donovan, K., Harrison, P., and Kelsall, R. W., "Self-consistent solutions to the intersubband rate equations in quantum cascade lasers: analysis of a GaAs/$AL_xGa_{1-x}As$ device," J. Appl. Phys. 89(6), 3084-3090 (2001).

[5] Haldar, M. K., "A simplified analysis of direct intensity modulation of quantum cascade lasers," IEEE J. Quantum Electron. 41(11), 1349-1355 (2005).

[6] Wang, C., Grillot, F., and Even J., "Impacts of wetting layer and excited state on the modulation response of quantum dot lasers," IEEE J. Quantum Electron. 48(9), 1144-1150 (2012).

[7] Yabre, G., "Effect of relatively strong light injection on the chirp-to-power ration and the 3 dB bandwidth of directly modulated semiconductor lasers," J. Lightwave Tech. 14(10), 2367-2373 (1996).

[8] Chen, F. H., Liu, M. J., and Simpson, B. T., "Response characteristics of direct current modulation on a bandwidth enhanced semiconductor laser under strong injection locking," Opt. Commun. 173, 349-355 (2000).

[9] Simpon, B. T., and Liu, M. J., "Bandwidth enhancement and broadband noise reduction in injection-locked semiconductor lasers," IEEE photon. Technol. Lett. 7(7), 709-711 (1995).

[10] Liu, M. J. *et al*, "Modulation bandwidth, noise and stability of a semiconductor laser subject to strong injection locking," IEEE photon. Technol. Lett. 9(10), 1325-1327 (1997).

[11] Meng, J. X., Chau, T., and Wu, C., M., "Improved intrincis dynamic distortions in directly modulated semiconductor lasers by optical injection locking," IEEE Trans. Microw. Theory Tech. 47(7), 1172-1176 (1999).

[12] Seo, H. J., Seo, K. Y., and Choi, Y. W., "Nonlinear distortion suppression in directly modulated DFB lasers by sidemode optical injection," Proc. IEEE MTT-S Int. microw. Symp. Dig. 1, 555-558 (2001).

[13] Naderi, N. A., Pochet, M., Grillot, F., Terry, N. B., Kovanis, V., and Lester, L. F., "Modeling the injection-locked behavior of a quantum dash semiconductor laser," IEEE J. Sel. Top. Quantum Electron. 15(3), 563-571 (2009).

[14] Simpson, B. T., and Liu, M. J., "Small-signal analysis of modulation characteristics in a semiconductor laser subject to strong optical injection," IEEE J. Quantum Electron. 32(8), 1456-1468 (1996).

[15] Simpson, B. T., and liu, M. J., "Enhanced modulation bandwidth in injection-locked semiconductor lasers," IEEE photon. Technol. Lett. 9(10), 1322-1324 (1997).

[16] Murakami, A., Kawashima, K., and Atsuki, K., "Cavity resonance shift and bandwidth enhancement in semiconductor lasers with strong light injection," IEEE J. Quantum Electron. 39(10), 1196-1204 (2003).

[17] Sirtori, C., Page, H., Becker, C., and Ortiz, V., "GaAs-AlGaAs quantum cascade lasers: physics, technology, and prospects," IEEE J. Quantum Electron. 38(6), 547-558 (2002).

[18] Sirtori, C., Nagle, J., "Quantum cascade lasers: the quantum technology for semiconductor lasers in the mid-far-infrared," C. R. Physique 4, 639-648 (2003).

[19] Capasso, F. *et al*, "Quantum cascade lasers: ultrahigh-speed operation, optical wireless communication, narrow linewidth, and far-infrared emission," IEEE J. Quantum Electron. 38(6), 510-532 (2002).

[20] Paiella, R., Martini, R., Capasso, F., and Gmachl, C., "High-frequency modulation without the relaxation oscillation resonance in quantum cascade lasers," Appl. Phys. Lett. 79(16), 2526 (2001).

[21] Barbieri, S., Maineult, W., Dhillon, S., S., Sirtori, C., and Alton, J., "13 GHz direct modulation of the terahertz quantum cascade lasers," Appl. Phys. Lett. 91(14), 143510 (2007).

[22] Maineult, W., Ding, L., Gellie, P., Filloux, P., and Sirtori, C., "Microwave modulation of terahertz quantum cascade lasers: a transmission-line approach," Appl. Phys. Lett. 96(2), 021108 (2010).

[23] Meng, B., and Wang, Q. J., "theoretical investigation of injection-locked high modulation bandwidth quantum cascade lasers," Optics Express 20(2), 1450-1464 (2012).

[24] Borri, S. *et al*, "direct link of a mid-infrared QCL to a frequency comb by optical injection," Optics Letter 37(6), 1011-1013 (2012).

[25] R. Lang, "Injection locking properties of a semiconductor laser," IEEE J. Quantum Electron. QE-18, 976-983 (1982).

[26] Rana, F., and Ram, R. J., "Current noise and photon noise in quantum cascade lasers," Physical Review B 65, 125313 (2002).
[27] Gensty, T., and Elsaber, W., "Semiclassical model for the relative intensity noise of intersubband quantum cascade lasers," Optics Communications 256, 171-183 (2005).
[28] Petitjean, Y., Destic, F., Mollier, J. C., and Sirtori, C., "Dynamic modeling of terahertz quantum cascade lasers," IEEE J. Sel. Top. Quantum Electron. 17(1), 22-29 (2011).
[29] Faist, J. *et al*, "Terahertz quantum cascade laser," Phil. Trans. R. Soc. Lond. A 362, 215-231 (2004).
[30] Sirtori, C., "Quantum cascade laser : fundamentals and performances," in Les lasers: applications aux technologies de l'information et au traitement des matériaux. Les Ulis, France : EDP Science (2002).
[31] Wieczorek, S., Simpson T. B., Krauskopf, B., and Lenstra, D., "Global quantitative predications of complex laser dynamics," Physical Review E 65, 045207 (2002).
[32] Wieczorek, S., Krauskopf, B., Simpson, T. B., and Lensra, D., "The dynamical complexity of optically injected semiconductor lasers,"Physics Reports 416, 1-128 (2005).
[33] Green, R. P., Xu, J.H., Mahler, L., Tredicucci, A., and Beltram, F., "Linewidth enhancement factor of terahertz quantum cascade lasers," Appl. Phys. Lett. 92(7), 071106 (2008).
[34] Aellen, T., Maulini, R., Terazzi, R., Hoyler, N., Giovannini, M., and Faist, J., "Direct measurement of the linewidth enhancement factor by optical heterodyning of an amplitude-modulated quantum cascade laser," Appl. Phys. Lett. 89(9), 091121 (2006).
[35] Staden, J. V., Gensty, T., and Elsaber, W., "Measurements of the α factor of a distributed-feedback quantum cascade laser by an optical feedback self-mixing technique," Optics Letters 31(17), 2574-2576 (2006).